

Combining double-layer arrays and metal film for zeroth order suppressing

ZHICHAO XIONG, BO WANG*, XIAOQING ZHU, YUSEN HUANG, LICHANG LI, JIAMAN HONG, YONGCHUN ZHOU

School of Physics and Optoelectronic Engineering, Guangdong University of Technology, Guangzhou 510006, China

In this paper, a reflective two-port beam splitter grating with zeroth order suppressed is proposed. Under normal incidence, the finite element method is chosen to optimize the grating parameters, and the results are verified by the rigorous coupled-wave analysis. In this study, the incident light wavelength is chosen as 1.55 μm . The grating reflective efficiency of 0th order is suppressed, and the diffraction efficiencies of ± 1 st orders attain 48.07% in transverse electric polarization and 47.40% in transverse magnetic polarization. What's more, the grating has the characteristic of high efficiency in a certain range of incident wavelength.

(Received November 8, 2021; accepted June 6, 2022)

Keywords: Two-port, Beam splitter, Reflective grating, Under normal incidence

1. Introduction

Beam splitter is one of the most basic diffractive optical components with the function of dividing the incident light into multiple beams. Beam splitter plays an important role in the fields of optoelectronic information processing [1-4], optical communication [5-8], laser systems [9-11], and optical detection [12,13], etc. Vector diffraction theory is the theoretical basis for the study of subwavelength gratings and resonance-domain gratings [14]. We can use finite element method (FEM) [15-19], rigorous coupled-wave analysis (RCWA) [20-25], modal method and so on to carry out numerical analysis when the grating period is close to the wavelength of incident light. Conventional beam splitter is complex to fabricate and difficult to achieve high efficiency. However, with the development of manufacturing processing, grating size has been reduced and the efficiency has been greatly improved. Researchers have also delved further into multi-channel beam splitter, such as multi-channel output beam splitter and polarization-selective beam splitter [26-30]. In recent years, a series of theoretical and experimental works about double-layer beam splitter have been proposed and implemented. Guo et al. designed a three-port beam splitter grating based on a double-slot fused silica with the average diffraction efficiency achieves more than 95% for transverse electric (TE) polarization [31]. Shu et al. proposed a reflective double-layer three-port beam splitter under normal incidence. For TE polarization and transverse magnetic (TM) polarization, the 0th and ± 1 st orders diffraction efficiencies are close to 31% [14].

In this paper, a two-port beam splitter with 0th order suppressed under normal incidence is proposed. The

parameters of the beam splitter are analyzed by FEM and verified by RCWA to obtain the optimal result. FEM not only has the characteristic of high computational accuracy, but also can adapt to analyze the gratings with a variety of complex shapes. Therefore, FEM has become an effective engineering analysis method. For the grating proposed in this paper, the diffraction efficiencies of ± 1 st orders for both TE polarization and TM polarization are over 47%. With polarization-independent property, the proposed two-port beam splitter grating has broad application prospects in the field of high-capacity optical communication systems [32].

2. The double-layer reflective grating for zeroth order suppressing

The two-dimensional and three-dimensional schematic diagram of the double-layer beam splitter grating are demonstrated by Fig. 1 obviously. As shown in Fig. 1, the grating consists of double-layer rectangular grating ridges, silver reflection layer and fused silica substrate. Among them, the upper grating ridge is made of SiO_2 with refractive index $n_1=1.45$. The material of the lower grating ridge is set as Ta_2O_5 , with refractive index $n_2=2$. The refractive index of silver reflector is $n_3=0.469-9.32i$ with the thickness of 0.1 μm . The substrate material is consistent with the upper grating ridge. After multiple iterations of data analysis, we obtained a series of optimized parameters. To minimize the 0th order diffraction and maximize the ± 1 st orders diffraction efficiencies of TE and TM polarizations, the thickness of the upper grating ridge is set as $h_1=0.4 \mu\text{m}$, and the

thickness of the lower grating ridge is set as $h_2=1.2 \mu\text{m}$. According to the grating equation, the period d should be set in the range of one and two times of the incident wavelength λ . Through FEM, the final optimization result of grating period is $d=2.48 \mu\text{m}$. In addition, after a series of calculations, the duty cycle f of the grating is set as 0.4. The optimal parameters of the proposed grating are listed in Table 1 integrally.

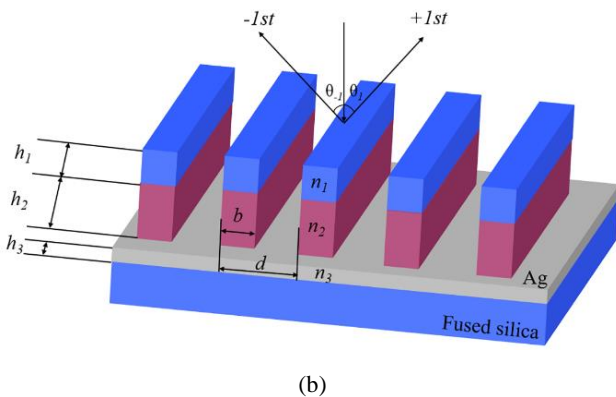
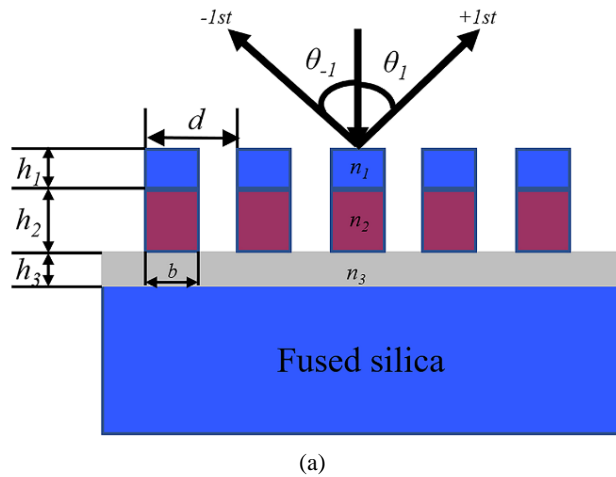


Fig. 1. The (a) two-dimensional and (b) three-dimensional schematic diagram of the double-layer beam splitter grating with 0th order suppressed under normal incidence (color online)

Table 1. The parameters of the double-layer beam splitter grating with 0th order suppressed

λ	d	f	h_1	h_2	h_3
1.55 μm	2.48 μm	0.4	0.4 μm	1.2 μm	0.1 μm

Fig. 2 shows the relationship between diffraction efficiencies and the thickness of grating ridge at different orders for TE and TM polarizations. Under normal incidence, according to the optimal parameters we obtained, the reflective efficiencies of 0th order for TE and TM polarizations are close to 0. This phenomenon has a positive effect on improving the diffraction efficiencies of $\pm 1\text{st}$ orders for TE and TM polarizations. It is illustrated the diffraction efficiencies of the grating obtained by FEM and RCWA for TE and TM polarizations at 0th order and $\pm 1\text{st}$ orders in Table 2, respectively.

Table 2. The reflective efficiencies of the grating obtained by FEM and RCWA for TE polarization and TM polarization with period $d=2.48 \mu\text{m}$, incident wavelength $\lambda=1.55 \mu\text{m}$, duty cycle $f=0.40$, $h_1=0.40 \mu\text{m}$, $h_2=1.20 \mu\text{m}$, $h_3=0.10 \mu\text{m}$

Polarization	0th	$\pm 1\text{st}$
TE (FEM)	0.69%	48.07%
TE (RCWA)	0.70%	48.07%
TM (FEM)	0.86%	47.40%
TM (RCWA)	0.92%	47.44%

According to Table 2, we can draw a distinct conclusion that the double-layer grating can separate the incident light into $\pm 1\text{st}$ orders for TE polarization with the efficiencies of 48.07% and for TM polarization with the efficiencies of 47.40%. Therefore, the grating serve as a two-port beam splitter with 0th order suppressed.

Fig. 3 demonstrates the normalized electric field distribution of the grating for TE and TM polarizations respectively, and we can obtain the energy distribution information of incident light from the figures obviously. Due to the periodic structure, the energy distribution in the grating also has the periodic characteristic. The energy of incident light is reflected by silver layer and distributed in the grating ridge and grating groove.

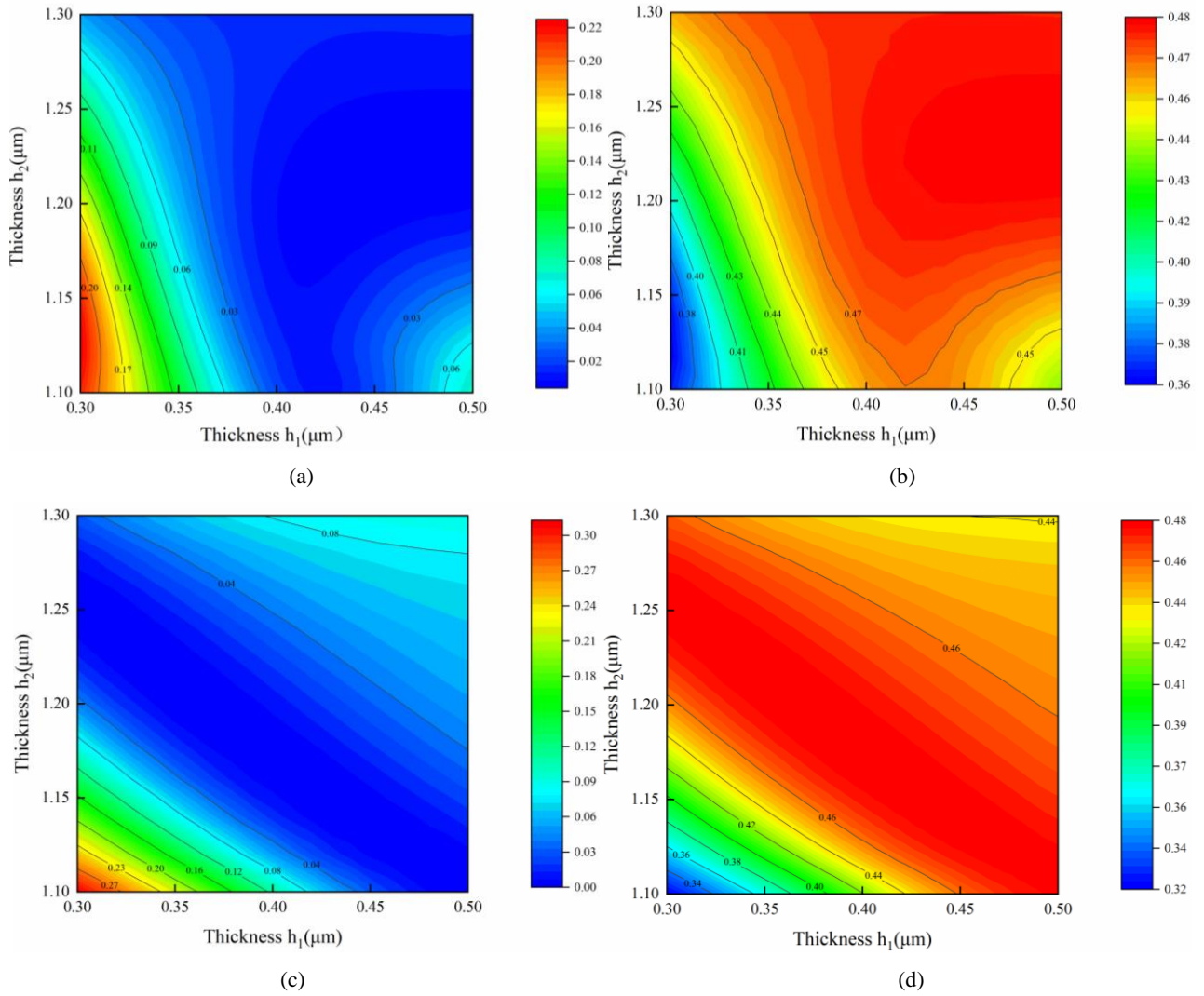


Fig. 2. The contour map of the relationship between reflective efficiencies and the depths of h_1 and h_2 for TE polarization and TM polarization with incident wavelength $\lambda=1.55 \mu\text{m}$, period $d=2.48 \mu\text{m}$, duty cycle $f=0.4$ under normal incidence: (a) 0th order for TE polarization, (b) ± 1 st orders for TE polarization, (c) 0th order for TM polarization, (d) ± 1 st orders for TM polarization (color online)

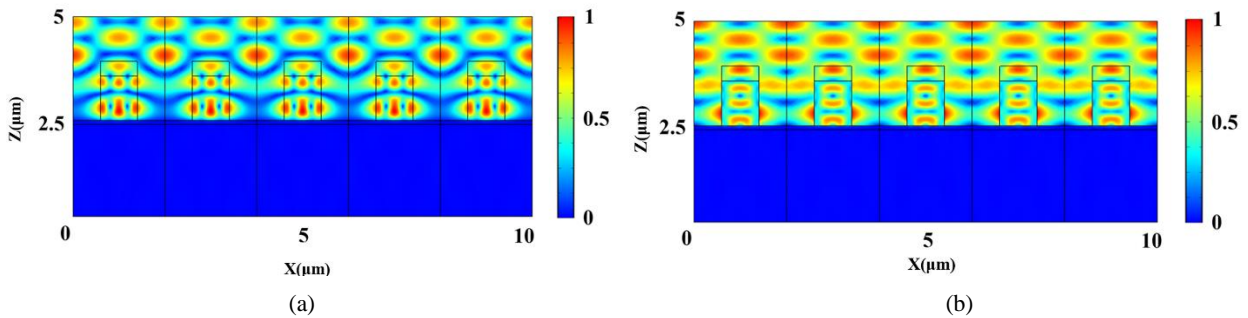


Fig. 3. The normalized electric field distribution with incident wavelength $\lambda=1.55 \mu\text{m}$, period $d=2.48 \mu\text{m}$, duty cycle $f=0.4$, $h_1=0.4 \mu\text{m}$, $h_2=1.2 \mu\text{m}$, $h_3=0.1 \mu\text{m}$: (a) TE polarization and (b) TM polarization (color online)

3. Analysis and discussions

As is well-known that the values of period, duty cycle and incident wavelength have a great influence in the diffraction efficiency of the grating. For the actual

manufacturing, the tolerance value of grating is worth to discuss. Firstly, the manufacturing process of this grating is introduced. The first step is to choose a dry and clean fused silica substrate, prepare a silver film with the

thickness of 0.1 μm , and cover the silver film on the substrate by evaporating and concentrating. Afterwards, covering the substrate with a layer of photoresist and recording the generated grating by holographic exposure and development. The next step is to transfer the grating model on the photoresist to a dichromate solution for chromium mask. Etching the grating into fused silica in an inductively coupled plasma instrument is a pivotal step. In addition, etching by ion beam is also a reliable fabrication method. The last step is to remove the remaining raster masks. The grating presented in this paper has the characteristics of simplicity and low cost in manufacturing process. The characteristics demonstrate that the grating has the potential for industrial production and practical application.

Fig. 4 demonstrates the relationship between diffraction efficiency and duty cycle. The value of duty cycle is determined by the manufacturing process. Nevertheless, some inaccuracy within certain range is permissible. It can be seen obviously from Fig. 4 that the diffraction efficiencies of $\pm 1\text{st}$ orders for TE and TM polarizations are best when the duty cycle is set as 0.4. It is worth noting that the diffraction efficiency of grating is still above 44% for TE polarization and 47% for TM polarization when the duty cycle is in the range of 0.39 to 0.41.

Besides, the values of incident wavelength make a great influence in the diffraction efficiencies for TE polarization and TM polarization. Fig. 5 depicts the relationship between incident wavelength and diffraction efficiencies for TE and TM polarizations under normal incidence. With a number of precise calculations, we can draw a definite conclusion that the diffraction efficiency of the reflective double-layer grating with 0th order suppressed will exceed 47% for TE polarization while the incident wavelength is in the range of 1.540 μm to 1.575 μm . In addition, the grating has a wider wavelength bandwidth for TM polarization when the wavelength is in the range of 1.5 μm to 1.6 μm . In this case, the diffraction efficiency of TM polarization is greater than 47%. The tolerance values of this grating are significantly better than the grating proposed in Ref. [14], which just achieved about 90% total diffraction efficiency at a bandwidth of $6 \times 10^{-3} \mu\text{m}$. The above parameters and data analysis result demonstrate clearly that the grating has the characteristics of high efficiency and wide bandwidth.

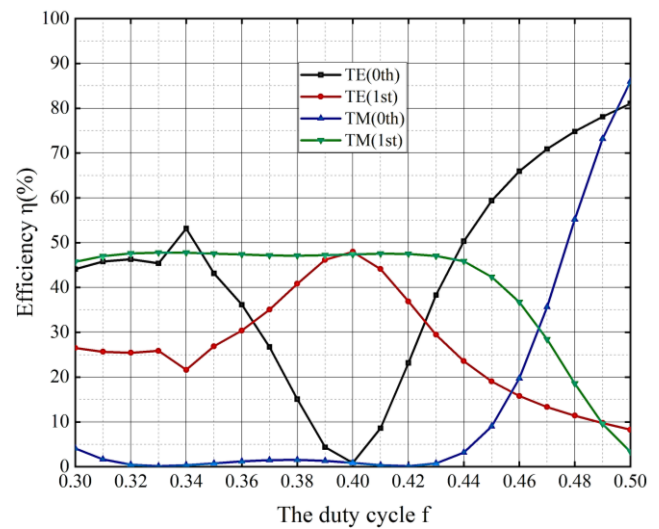


Fig. 4. The efficiency corresponding to the duty cycle f at wavelength of 1.55 μm with period of 2.48 μm under normal incidence (color online)

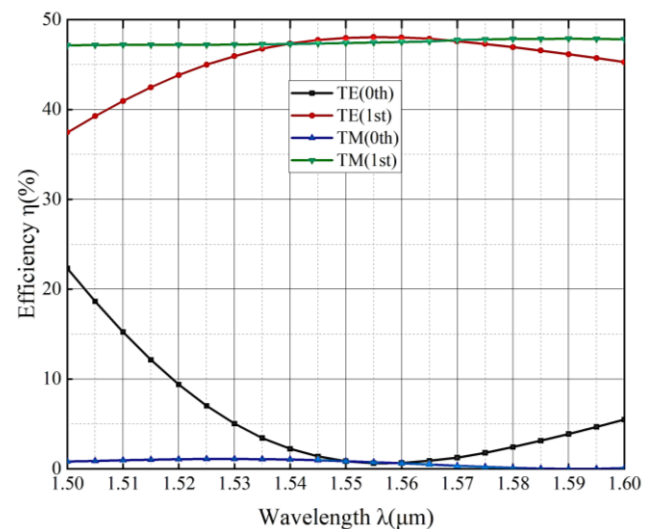


Fig. 5. The efficiency corresponding to the incident wavelength with duty cycle of 0.4 and period of 2.48 μm under normal incidence (color online)

What's more, period is also a major factor affecting the diffraction efficiency of the grating. Therefore, it is necessary to research the period to improve the grating performance. The reflective efficiency versus period is displayed in Fig. 6. On the grounds of the calculate results from FEM and verified by RCWA, the diffraction efficiency is greatest when the period is 2.480 μm . It is worth noting that in the range of 2.435 μm to 2.495 μm , the efficiencies of $\pm 1\text{st}$ orders for TE and TM polarizations are greater than 47.09%. Meanwhile, the 0th order diffraction efficiency of the grating is less than 2.4%.

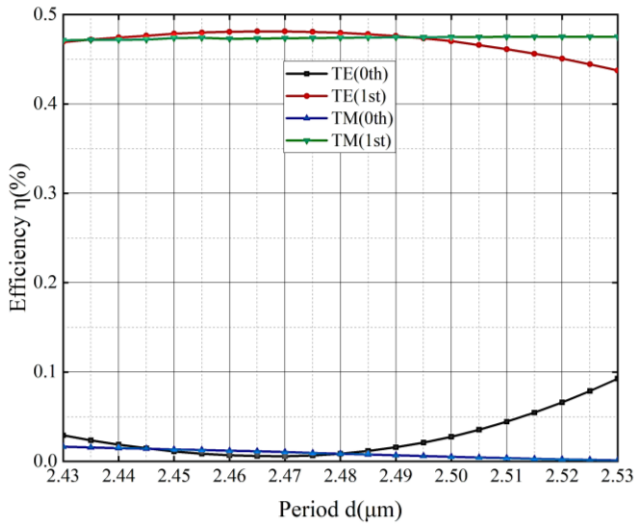


Fig. 6. The diffraction efficiency corresponding to the period at wavelength of $1.55 \mu\text{m}$ and duty cycle of 0.4 under normal incidence (color online)

In the end, the properties of the silver reflector are of interest. Firstly, after rigorous calculation, the refractive efficiency in TE and TM polarizations is too small and can be approximated to 0. So, the absorption of silver reflective layer is equal to one minus the total reflection efficiency. The total reflection efficiency is equal to the efficiency of 0th order plus the efficiencies of ± 1 st orders respectively. So, after a simple calculation, it's not hard to figure out that the absorption of silver reflector at wavelength of $1.55 \mu\text{m}$ with duty cycle of 0.4 and period of $2.48 \mu\text{m}$ under normal incidence is 3.17% for TE polarization. Similarly, we can obtain that the absorption efficiency of the silver reflector for TM polarization is 4.34% . The above data indicate that the silver reflector is absorbent.

The effect of silver thickness on the grating reflection efficiency is discussed below. Fig. 7 depicts the relationship between diffraction efficiency and the thickness of reflecting layer h_3 . It can be clearly seen from the figure that the diffraction efficiency is constant when the thickness of the silver reflective layer is changing constantly in the range of $0.1 \mu\text{m}$ to $1 \mu\text{m}$. The figure demonstrated that the thickness of the silver reflector has little effect on the diffraction efficiency of the grating. It has a positive effect on improving the reflectivity of the grating.

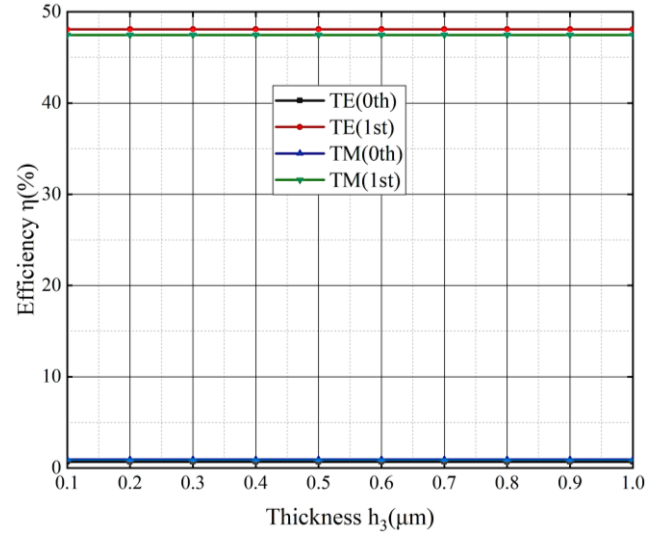


Fig. 7. The efficiency corresponding to the reflecting layer thickness h_3 at wavelength of $1.55 \mu\text{m}$ with duty cycle of 0.4 and period of $2.48 \mu\text{m}$ under normal incidence (color online)

4. Conclusion

A reflective double-layer grating with 0th order suppressed under normal incidence is proposed in this paper. According to FEM and RCWA, the optimized parameters of the grating are calculated, and the results are satisfactory. For TE polarization, the efficiencies of ± 1 st orders are greater than 48% . In the meantime, the diffraction efficiencies of ± 1 st orders for TM polarization attain 47.4% . Meanwhile, the diffraction efficiencies of 0th order for TE and TM polarizations are close to 0. Moreover, the relationship between diffraction efficiency and duty cycle, incident wavelength, period and the thickness of reflecting layer are researched to obtain the optimal parameters. The parameters and data analysis results reveal that this paper proposed a two-port zeroth-elimination beam splitter with satisfactory performance. In addition, the proposed grating has the characteristic of broad incident wavelength bandwidth for TE and TM polarizations.

Acknowledgements

This work is supported by the National Natural Science Foundation of China (62131018) and the Science and Technology Program of Guangzhou (202002030284, 202007010001).

References

- [1] W. Yu, Y. Tian, S. Zhang, W. Tan, *Optik* **220**, 165141 (2020).
- [2] F.-Q. Dou, Z.-M. Yan, X.-Q. Liu, W.-Y. Wang, C.-C. Shu, *Optik* **210**, 164516 (2020).
- [3] Y. Gao, H. Song, S. Geng, M. Jin, *Opt. Eng.* **60**(5), 057105 (2021).
- [4] J. Wang, Q. Jiang, D. Han, *Results Phys.* **24**, 104084 (2021).
- [5] Z. Lin, B. Wang, *Opt. Eng.* **60**(4), 045108 (2021).
- [6] Y. Chen, X. Zhou, M. Zhang, *Phys. Lett. A* **384**(34), 126877 (2020).
- [7] F. Bucholtz, J. Singley, *Opt. Eng.* **59**(12), 120801 (2020).
- [8] U. F.S. Roggero, H. E. Hernández-Figueroa, *Opt. Laser Technol.* **127**, 106127 (2020).
- [9] J. Ding, L. Huang, W. Liu, Y. Ling, W. Wu, H. Li, *Opt. Express* **28**(22), 32721 (2020).
- [10] T. Dong, J. Lin, Y. Zhou, C. Gu, P. Yao, L. Xu, *Opt. Laser Technol.* **136**, 106740 (2021).
- [11] C. Shan, X. Zhao, Y. Gao, Y. Zhao, D. Rao, Y. Cui, C. Li, G. Hu, W. Ma, Z. Sui, J. Shao, *Opt. Laser Technol.* **130**, 106368 (2020).
- [12] X. Gao, Q. Wang, S. Cao, R. Li, R. Hong, D. Zhang, *Opt. Express* **28**(17), 25073 (2020).
- [13] T. Dong, B. Gao, S. Chen, Z. Zhang, X. Cui, C. Jiang, C. Zhao, *Opt. Commun.* **498**, 127202 (2021).
- [14] W. Shu, B. Wang, H. Li, L. Lei, L. Chen, J. Zhou, *Superlattices Microstruct.* **85**, 248 (2015).
- [15] W. Zeng, Y. Yao, S. Qi, L. Liu, *Optik* **207**, 163812 (2020).
- [16] W. Zeng, X. Zou, Y. Yao, *Optik* **224**, 165733 (2020).
- [17] A. Aminzadeh, A. Parvizi, M. Moradi, *Opt. Laser Technol.* **125**, 106029 (2020).
- [18] N. Yang, J. Xiao, *Opt. Commun.* **459**, 125095 (2020).
- [19] E. Elashamla, S. Hekal, L. Gomaa, *Opt. Commun.* **457**, 124621 (2020).
- [20] G. Wu, Y. Huang, X. Duan, K. Liu, X. Ma, T. Liu, H. Wang, X. Ren, *Opt. Commun.* **456**, 124458 (2020).
- [21] Y. Li, B. Lin, M. Hu, D. Pang, *Opt. Commun.* **455**, 124567 (2020).
- [22] B. Wang, L. Chen, L. Lei, J. Zhou, *IEEE Photon. Technol.* **25**(9), 863 (2013).
- [23] Y. Chen, J. Xiao, *Opt. Eng.* **59**(1), 017101 (2020).
- [24] Z. Zhang, F. Wang, J. Song, Y. Zhao, *Chin. Phys. B* **29**(2), 020503 (2020).
- [25] Z. Xu, T. Lyu, X. Sun, *Opt. Commun.* **451**, 17 (2019).
- [26] Y. Xie, Z. Chen, Y. Wu, Y. Zhao, T. Huang, Z. Chang, *Opt. Eng.* **58**(9), 095102 (2019).
- [27] Z. Lyu, C. Wang, Y. Pan, R. Xia, T. Chen, L. Sun, *Opt. Lett.* **44**(8), 2129 (2019).
- [28] H. Huang, T. Zhai, Q. Song, X. Yin, *Opt. Commun.* **434**, 28 (2019).
- [29] B. Wang, L. Lei, L. Chen, J. Zhou, *Opt. Commun.* **285**(21), 4599 (2012).
- [30] T. Sharma, V. Rana, J. Wang, Z. Cheng, *Optik* **227**, 165995 (2021).
- [31] L. Guo, X. Liu, X. Ge, *Optik* **202**, 163569 (2020).
- [32] Z. Lin, B. Wang, *Laser Phys.* **31**(2), 026202 (2020).

*Corresponding author: wangb_wsx@yeah.net